



## Gas sensing and dielectric properties of TiO<sub>2</sub>/Stilbite nanocomposites

Vikas Kutte<sup>a</sup>, Kishori Naik<sup>b</sup>, Madhuri Lakhane<sup>c</sup>, Malikarjun Wakade<sup>d</sup>, Pankaj Waghmare<sup>b</sup>, Pandurang Sabale<sup>e</sup>, Megha Mahabole<sup>b,\*</sup>

<sup>a</sup>Yeshwant Mahavidyalaya, Nanded 431602, India

<sup>b</sup>Swami Ramanand Teerth Marathwada University, Nanded 431606, India

<sup>c</sup>DSM College, Parbhani 431401, India

<sup>d</sup>Shivneri Mahavidyalaya, ShirurAnantpal 413544, India

<sup>e</sup>Deccan College, Pune 411004, India

### ARTICLE INFO

#### Article history:

Available online 15 May 2023

#### Keywords:

Ammonia  
Composite  
Dielectric  
Gas sensor  
Stilbite  
TiO<sub>2</sub>  
Etc

### ABSTRACT

The present work deals with the detection of ammonia gas by using TiO<sub>2</sub>/Stilbite composites. It also presents the dielectric properties of Stilbite and its composites. The composites are prepared by using Stilbite as a main matrix and TiO<sub>2</sub> metal oxide as a filler material with variable wt% via mechanical mixing method. The prepared composites material are characterized by XRD, FTIR technique. The XRD and FTIR pattern of composites ensure the presence of TiO<sub>2</sub> in composites. The thick film of TiO<sub>2</sub>/stilbite composites prepared by using screen printing technique are used to detect ammonia gas. The sensing parameter such as operating temperature, response/recovery time, transient response and gas uptake capacity have been determined. In addition, dielectric properties of composites, in pellets form are studied. The sensitivity of ammonia gas sensing increasing as increase the TiO<sub>2</sub> concentration in composites. In addition, dielectric constant of composites are also increases as function of TiO<sub>2</sub> concentration.

Copyright © 2023 Elsevier Ltd. All rights reserved.

Selection and peer-review under responsibility of the scientific committee of the 2nd International Conference on Multifunctional Materials.

### 1. Introduction

The issue related to environmental pollution is becoming graver with the industrial development and urbanization [1]. Therefore, considerable attention has to be given on air pollution. It is observed that the toxic gases which are engendered from various industries, vehicles and chemical waste have harmful effects on human beings. Among various gases, gaseous ammonia, the most abundant alkaline gas in the atmosphere, is a colorless, pungent, highly toxic, and corrosive gas [2]. Agriculture, animal husbandry and fertilizers are the key sources of ammonia emission in addition to sources like trade processes, volatilization from soils and oceans [3]. Nowadays studies have detected that the rate of ammonia emission is increasing over the last few decades. Though, ammonia gas is essential in nitrogen fertilizers production, refrigeration, manufacturing units, refining operations and cleaning in accordance with an Occupational Safety and Health Administration report, very small amount of ammonia can cause irritation to the

eyes, nose and throat. Even direct contact of concentrated ammonia can cause serious injury [4]. Higher concentrations of ammonia may cause blindness, seizures, lung disease, damage to the nervous system and even death. Furthermore, ammonia leads to the formation of atmospheric particulate matter which results in dilapidation in visibility and atmospheric deposition of nitrogen, being a major component of total reactive nitrogen, may acutely affect ecosystems. Thus, the increase in ammonia emissions may lead to undesirable impact on and public and climate health as well as environmental [5]. Hence, in order to safeguard human hazards and the surrounding environment, detection of ammonia is very important. So, there is an urgent need to develop a kind of gas sensor with high sensitivity that can sense ammonia at low temperature.

Zeolites are crystalline aluminosilicates involving group IA and IIA elements. They are porous solids belonging to molecular sieve group [6]. Structurally, zeolites are very complex exhibiting three-dimensional framework developed by the linkages between AlO<sub>4</sub> and SiO<sub>4</sub> tetrahedron (TO<sub>4</sub> building block; T = Al or Si) via sharing of oxygen ions. Hence, structure comprises of channels, interconnected voids and cages. They possess exceptional proper-

\* Corresponding author.

E-mail address: [mpmsrtmunsp@gmail.com](mailto:mpmsrtmunsp@gmail.com) (M. Mahabole).

ties namely extraordinary adsorption ability, excellent ion exchange capability, catalytic selectivity and molecular sieving nature [7]. It is due to open, infinite, highly porous and three dimensional & rigid crystal structure. Zeolites are widely being employed in various sectors viz agriculture, catalysis, chromatography, waste water treatment, and sensor [8]. Zeolites have been grouped into two main categories namely natural and synthetic [9]. However, natural zeolites are preferred than synthetic form because of various factors such as large-scale natural prosperity,

Significant surface area, high thermal stability, user-friendliness and low cost [10]. Stilbite is secondary hydrothermal mineral which exists in two forms; Ca-Stilbite and Na-Stilbite[11]. The framework of stilbite, called as STI framework, composed of two kinds of interconnecting channels; 8-ring channels along the [101] direction and bigger 10-ring channels parallel to the [100] direction along with a cavity formed at the intersection of these channels. Literature survey reflects that stilbite is widely used as an adsorbent for waste water treatment and removal of fluoride from drinking water [12]. Cesium cation exchange and natural stilbite zeolite's cation selectivity have both been performed by Baek. [13]. Kiseleva and co-workers have carried out the thermochemical and calorimetric measurements of stilbite zeolites [14]. O. Schaf have utilized stilbite single crystals to detect methanol, propanol and 3-pentanol with the aid of impedance spectroscopy by the determination of electrical properties [15].

Since porous nature of stilbite leads to large surface area and high adsorption capability, which are the key requirements for any sensor, considerable attention has been given on stilbite for sensor application. Being of natural origin, stilbite is easily available. It shows environmental compatibility, stability and ability to form composites. Hence, in our earlier work, the thick films of stilbite and its composites with a blending of ZnO, TiO<sub>2</sub> and CuO metal oxide materials have been developed for detection of ethanol vapours with improved sensor properties. Furthermore, no reports are available for stilbite and stilbite-based composites for detection of ammonia so far.

Literature survey reflects that many metal oxides have been tested for detecting other combustive, oxidizing and reducing gases including ammonia [16–18]. Since the previous few decades, TiO<sub>2</sub> based gas sensors in particular have drawn a lot of interest because of their high thermal stability, good resistance to harsh climatic conditions and ecologically favourable features [19]. TiO<sub>2</sub> sensors, with different nano-structural morphologies, have exhibited much higher sensitivity, selectivity and long term stability for ammonia [20]. Therefore, TiO<sub>2</sub> has been chosen as a filler to prepare composite sensor.

However, most of metal oxide sensors work at higher operating temperature with only few exceptional sensors operating at room or low temperatures. On the other hand, sensors based on zeolite materials work at somewhat low temperatures ensuring low power consumption but face a problem of high response/recovery time compared with metal oxide sensors. To overcome the limitations mentioned above, the combination of TiO<sub>2</sub> metal oxide and stilbite have been developed and tested for the detection of ammonia gas to achieve excelsior performance in continuation with earlier work.

Furthermore, zeolites belong to dielectric material category. It exhibits energy storage when an external electric field is applied. The complex electrical and dielectric properties of zeolites have been the subject of immense studies for last decades. While considerable research has been done on the dielectric characteristics of different zeolites, including ZSM-5, Na-X, Na-Y, Ca-A, natural, Ba2+ -doped and electron irradiated clintonite, pure silica films, HY, ALPO<sub>4</sub>, LDPE/4A zeolite composite, metal oxides/ZSM-5, no detailed work of the effects of addition of TiO<sub>2</sub> on the dielectric

properties of stilbite at different frequencies has been carried out so far [21–25].

Therefore, this study is particularly aimed to present the ammonia sensing performance of pristine stilbite films and the augmented response capabilities of gas sensors based on TiO<sub>2</sub>/Stilbite composite films. All sensors are tested as a function of temperature, time and ammonia concentration. In addition, dielectric study on stilbite composites was also carried out. The experimental findings on the dielectric performance of three composites as a function of ac field frequency have also been demonstrated in this paper.

## 2. Materials and method

### 2.1. Preparation of composites

For preparation of composites, stilbite mineral collected from queries from Ahmednagar district and commercially available TiO<sub>2</sub> (Merck grade) were used without further purification process. Using a straightforward physical mixture technique, TiO<sub>2</sub> metal oxide nanoparticles with 25%, 50% and 75% weight content of stilbite were made into particle reinforced composites. Thus initially, stilbite and TiO<sub>2</sub> powders, for a given combination, were weighed and to create uniform admixtures and ensure that metal oxides in zeolite were dispersed at various quantities, these materials were mechanically fully dry mixed for around 10 h.

### 2.2. Preparation of thick film sensor

Screen printing technique was employed for the preparation of thick films. By combining the right amount of functional material (stilbite and composites) with binders such as glass frit, butyl carbamate, and ethyl cellulose while maintaining a 70:30 inorganic to organic ratio, the thixotropic paste was created. The thick films of stilbite and TiO<sub>2</sub> based composites were screen printed on the pre-cleaned glass substrates having area (1 cm × 2 cm) and in order to achieve the necessary adhesion, the films were sintered at a temperature of 650 °C for 2 hrs. These screen-printed thick films were tested as sensor films to detect ammonia in further study.

### 2.3. Preparation of pellet

The sample powder was uniaxially pressed at 5 tonnes of pressure with a binder to produce a compact pellet with a 13 mm diameter and a 2 mm thickness for dielectric measurements. Finally, the pellets underwent a 2-hour heat treatment at 500 °C to completely remove the binder before being cooled to room temperature. To establish good electrical connections, the silver conducting paint was sprayed to both of the flat sides of the pellet, which was then utilized as a dielectric sample for further dielectric research.

### 2.4. Characterization

The prepared composites were characterized by using XRD and FTIR techniques. XRD spectra of composite samples were obtained by using Rigaku X-ray diffractometer with CuK $\alpha$  radiation (1.5432 Å<sup>0</sup>). The XRD spectra were recorded in the 2 $\theta$  range of 5–60° are recorded by using X-ray diffractometer. Shimadzu make FTIR spectrometer was used to obtain FTIR spectra of stilbite and composites with a scan range of 4000–400 cm<sup>-1</sup> and resolution of 4 cm<sup>-1</sup>.

## 2.5. Gas sensing characteristic studies

The gas sensing characteristics of stilbite and composite films, deposited by using screen printing technique, were studied by using a fixed volume gas chamber. The films were placed on a heater present in chamber. The temperature of heater and consequently of films was controlled by using dimmer-stat and detected by thermo-couple. The temperature of the sensor was increased room temperature to 300 °C. Initially, the output voltage was measured, across reference resistance joined in series with the sensor film, as a function of temperature and resistance of sensor film was determined as a function of temperature in air. Fixed amount of ammonia (50 ppm) was inserted into the gas chamber by using a syringe through small opening. The resistance of the sensor was noted in gaseous environment. The response (sensitivity) of the sensor is nothing but the relative percentage change in resistance of sensor of film and was determined with the help of following equation:

$$\text{Sensitivity}(R)\% = \frac{R_g - R_a}{R_a} \times 100$$

Where  $R_g$  is resistance of sensor film in (ammonia + air) and  $R_a$  in air atmospheres. The temperature at which the sensor film gives maximum response is known as the operating temperature of the sensor. It is determined by plotting response to ammonia as function of temperature. The operating temperature of each sensor was verified using a repeatability test. Response and recovery time of sensor film were also determined by exposing the sensors to air and (air + ammonia) environments alternately. The ammonia uptake capacity of each sensor film was also studied by exposing sensor to variable concentrations of ammonia at its operating temperature.

## 2.6. Dielectric studies

In the present study, the dielectric measurements of stilbite and  $\text{TiO}_2$  blended stilbite composites were carried out at room temperature. Prior to measurements, electric contacts were deposited by coating a silver paste on both the surfaces of the pellet samples. Using a QuadTech LCR 7600 frequency metre, the dielectric measurements were made between 10 Hz and 2 MHz. As a function of frequency, the  $C_p$ ,  $D_f$ ,  $R_s$ , and  $X_s$  were recorded and dielectric constant was calculated using the formula given below.

$$\epsilon' = \frac{C_p \times t}{\epsilon_0 \times A} \quad (1)$$

Where  $A$  is the area of the cross section of the sample pellet,  $C_p$  is the capacitance of the sample,  $t$  is its thickness,  $\epsilon_0$  is the permittivity of free space.

AC conductivity was calculated using the following formula;

$$\sigma = \frac{(Z')^2}{(Z')^2 + (Z'')^2} \times \frac{t}{A} \quad (2)$$

where  $Z'$  is the real part of impedance,  $Z''$  is the imaginary part of impedance,  $t$ -thickness of plate and  $A$ -Area of pellet.

The changes in dielectric constant, AC conductivity were plotted as a function of frequency. As a function of metal oxide content in a composite, the Cole-Cole plots were also shown and discussed.

## 3. Results and discussion

### 3.1. XRD analysis

The XRD pattern of stilbite,  $\text{TiO}_2$ /stilbite composites, and pure  $\text{TiO}_2$  samples are shown in Fig. 1 (a-e). Fig. 1(a) presents an XRD

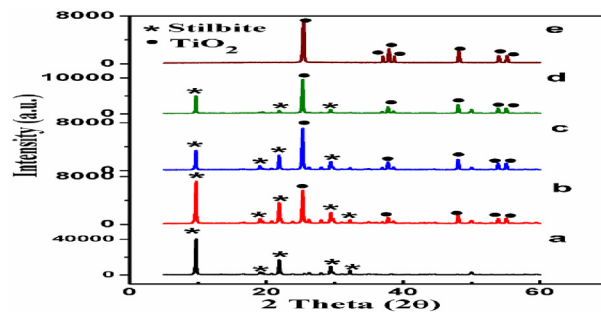


Fig. 1. XRD profile of stilbite,  $\text{TiO}_2$  and its composites.

pattern for pure stilbite and it is considered as the base. The stilbite characteristic peaks are found to be present at  $2\theta$  values of  $9.7^\circ$ ,  $19.08^\circ$ ,  $21.88^\circ$ ,  $29.38^\circ$  and  $32.24^\circ$  corresponding to (020), (220), (041), (060) and (260) planes for stilbite and are in good agreement with the standard and the literature data [23]. Thus, it can be concluded that zeolite samples collected from the queries are stilbite zeolites.

The XRD pattern for pure  $\text{TiO}_2$  (Fig. 1(e)) depicts the appearance of typical  $\text{TiO}_2$  peaks at  $2\theta$  values of  $25.28^\circ$ ,  $36.94^\circ$ ,  $37.90^\circ$ ,  $38.57^\circ$ ,  $48.2^\circ$ ,  $53.8^\circ$  and  $55.2^\circ$  corresponding to planes (101), (103), (004), (112), (200), (105) and (211) respectively.

Fig. 1(b-d) shows the XRD patterns of  $\text{TiO}_2$ /stilbite composites as a function of  $\text{TiO}_2$  concentration. These patterns reveal the presence of odd  $\text{TiO}_2$  peaks alongside the host stilbite peak. With an increase in  $\text{TiO}_2$  percentage, the prominent peaks corresponding to stilbite become less intense. For the maximum  $\text{TiO}_2$  concentration (75%), the stilbite peaks that appeared at  $19.08$  and  $32.24$  vanish. The composites' appearance of typical  $\text{TiO}_2$  peaks is proof that  $\text{TiO}_2$  has been incorporated into the stilbite matrix.

It can be inferred from the XRD study of  $\text{TiO}_2$ /stilbite composites that the XRD profiles exhibit the typical structural properties associated with the  $\text{TiO}_2$  and stilbite host. The superimposition of the XRD peaks for  $\text{TiO}_2$  and stilbite in each composite reveals the physical combination of their component parts and also validates the dispersion of  $\text{TiO}_2$  in the stilbite matrix. Phase analysis, performed by indexing data for  $\text{TiO}_2$  and stilbite, demonstrates that their crystal structures are intact in the composite and the primary matrix and the reinforcing substance don't interact chemically. Additionally, no novel phase structure is seen.

### 3.2. FTIR analysis

Fig. 2(a-e) displays the FTIR spectra of Stilbite,  $\text{TiO}_2$ /stilbite composites, and  $\text{TiO}_2$ . The FTIR spectrum for pure stilbite is displayed in Fig. 2(a) and it is considered as reference. The hydroxyl group is responsible for the occurrence of absorption bands at

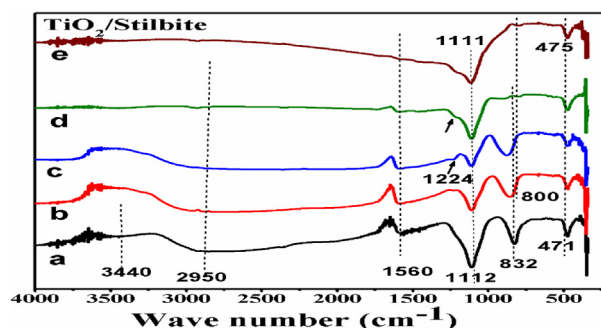


Fig. 2. FTIR spectra Stilbite,  $\text{TiO}_2$  and its composites.

3440 and 2950  $\text{cm}^{-1}$ . The bending mode of the  $\text{H}_2\text{O}$  molecule is responsible for the peak at 1560  $\text{cm}^{-1}$ . The T-O asymmetric stretching mode corresponds to the intense vibrations at 1112  $\text{cm}^{-1}$ . T-O bending vibrations are discovered to exist at 471  $\text{cm}^{-1}$  (T = Al or Si). The symmetric stretching motions of external linkages are attributed to the peak at 832  $\text{cm}^{-1}$  [26]. Thus, the FTIR results confirm the key functional groups for stilbite.

The Fig. 2 (e) represents the spectrum of pure  $\text{TiO}_2$  with the absorption peaks at 475, 800 and 1111  $\text{cm}^{-1}$ . The Ti-O-Ti framework bonds are attributed to the bands at 475 and 1111  $\text{cm}^{-1}$ . The symmetric stretching vibration of the Ti-O bonds in the  $\text{TiO}_2$  lattice is responsible for a peak of extremely low intensity that is present at about 800  $\text{cm}^{-1}$ . [26]. The FTIR spectra of  $\text{TiO}_2$ /Stilbite composites are shown in Fig. 2(b-d), where the appearance of Stilbite peaks at 471  $\text{cm}^{-1}$ , 832  $\text{cm}^{-1}$ , 1112  $\text{cm}^{-1}$ , 1560  $\text{cm}^{-1}$  and 2950  $\text{cm}^{-1}$  are gradually pushed toward the higher wavenumber side. As the Stilbite matrix's  $\text{TiO}_2$  concentration rises, a new peak is seen at 1224  $\text{cm}^{-1}$  as a result of the Ti-O stretching band and the band's disappearance from the Stilbite at 3440  $\text{cm}^{-1}$ . [28]. The spectra for  $\text{TiO}_2$ / Stilbite composites are depicted in Fig. 2(b-d). In this case also gradual shifting of stilbite peaks from 2950  $\text{cm}^{-1}$  and 1560  $\text{cm}^{-1}$  to higher wave numbers is observed. The band at 3440  $\text{cm}^{-1}$  vanishes for higher  $\text{TiO}_2$  concentration. The absorbance at 1112  $\text{cm}^{-1}$  and 471  $\text{cm}^{-1}$  goes on decreasing with higher  $\text{TiO}_2$  concentration up to 50% and for still higher concentration (75%), increase in absorbance is revealed. This may be due to the overlapping of  $\text{TiO}_2$  and stilbite peaks. The emergence of new shoulder peak, attributed to Ti-O stretching band, can also be observed at about 1224  $\text{cm}^{-1}$  for composites. It is also observed that with the increasing concentration of  $\text{TiO}_2$ , the absorbance for a peak at 832  $\text{cm}^{-1}$  goes on decreasing. The spectra are self-explanatory indicating the successful incorporation of  $\text{TiO}_2$  into the stilbite matrix.

### 3.3. Gas sensing analysis

Fig. 3 (a) presents the variation in sensitivity for pure stilbite film as a function of temperature for a fixed ammonia concentration. The graph shows the repetitive nature wherein maximum sensitivity (17250) is observed at 50°C. This confirms the working temperature of stilbite sensor. In order to enhance the sensor performance,  $\text{TiO}_2$  was incorporated in the stilbite matrix. The effect of addition of  $\text{TiO}_2$  on response and operating temperature is shown in Fig. 3(b-d). The operating temperatures of  $\text{TiO}_2$ /Stilbite composites with 25%, 50% and 75%  $\text{TiO}_2$  contents are found to be 35 °C, 35 °C, 40 °C respectively. The comparative response of  $\text{TiO}_2$ /Stilbite composite sensor thick films to the known amount of ammonia (50 ppm), presented in Fig. 3(e), shows a decrease in working temperature. The composite with 75%  $\text{TiO}_2$  exhibits maximum sensitivity (89423). It is clear that addition of  $\text{TiO}_2$  in stilbite changes not only the operating temperature but also sensitivity for ammonia gas. Therefore, it can be concluded that operating temperature and sensitivity are the functions of  $\text{TiO}_2$  concentration for composites (See Table 1).

Gas sensing is a surface phenomenon. When sensor is exposed to target gas, the gas molecules get adsorb on the surface and interacts with adsorbate molecules. This results in change in resistance and ultimately change in sensitivity. The more the number of active sites available on the surface, the higher will be the adsorption probability and consequently higher sensitivity. The number of active sites depends on the sensor sample. Hence, change in operating temperatures for various sensors ensures the more of adsorption sites at that temperature compared to other temperatures. Therefore, working temperatures for samples are different. Variation in sensitivity for specific sensor indicates availability of active sites at that temperature.

Fig. 4. shows the variation in response for Stilbite and  $\text{TiO}_2$  /Stilbite composites as a function of time. It is found that Stilbite has response and recovery times of 540 s and 60 s, respectively. The response and recovery time for  $\text{TiO}_2$  /Stilbite composites are observed to be the function of  $\text{TiO}_2$  concentration in composites. The response times for 25%, 50% and 75%  $\text{TiO}_2$  contents in composites are 360sec, 294sec and 223 sec respectively. It is observed that the higher the  $\text{TiO}_2$  concentration, the lower the response time. It is observed that recovery times also depend on  $\text{TiO}_2$  concentration. The recovery time decreases with increase in  $\text{TiO}_2$  amount in composites. The pure stilbite gets recovered quickly within one minute compared to composites. Therefore, it can be said that blending of  $\text{TiO}_2$  in Stilbite augments the response time although recovery is slightly higher.

Fig. 5. shows the transient behaviour of stilbite and composite film sensors. Stilbite film can sense 100 ppm ammonia. For still higher concentration the sensor saturates. Hence, stilbite sensor film is exposed to 30 ppm, 50 ppm and 70 ppm ammonia gas concentrations as depicted in inset. The stilbite composite films are exposed to 50 ppm, 100 ppm and 150 ppm ammonia gas concentrations. It is observed that response to ammonia increases with increase in ammonia concentration. All samples show the same trend.

The change in response with ammonia concentration is presented in Fig. 6. Initially the response increases linearly with low ammonia concentration. For further increase in ammonia concentration, it gets saturated. All samples exhibit the same behaviour. Stilbite can detect ammonia only up to 100 ppm whereas composite with 75%  $\text{TiO}_2$  can sense ammonia with higher concentration of 1300 ppm. These results indicate that uptake capacity of a sensor can be improved by  $\text{TiO}_2$  impregnation. At low concentration, the only few adsorption sites get occupied by gaseous species. As the concentration increases, more and more sites get occupied. For further higher concentration, no sites are available for adsorption to take place as almost all sites are already occupied. It results in saturation.

### 3.4. Dielectric analysis

Fig. 7(a-c) show the variations in dielectric constant for stilbite and composite materials as a function of frequency of applied field, with the dielectric constant for stilbite serving as the reference. It should be noticed that the dielectric constant ( $\epsilon'$ ) rapidly drops as applied frequency rises in the low frequency range before nearly remaining constant at higher frequencies. All of the composite samples show the same pattern.

It is discovered that a pure stilbite sample has a dielectric constant of 14. Stilbite and  $\text{TiO}_2$  together produce exceptionally high dielectric constants. It should be noted that a composite with 25%  $\text{TiO}_2$  has a dielectric constant on the order of 28454, which is 2000 times higher than the dielectric constant of pure stilbite. Highest value of dielectric constant (87094) is exhibited for the highest  $\text{TiO}_2$  concentration (75%) as depicted in Fig. 7.

Fig. 8(a-d) shows the plot of real impedance ( $Z'$ ) Vs imaginary impedance ( $Z''$ ) taken over a frequency range of 20 Hz-1 MHz. The X-axis specifies real part of the impedance ( $Z'$ ) and the Y-axis indicates imaginary part of the impedance ( $Z''$ ). The cole-cole plot for pure stilbite exhibits a single semi-circular behaviour in low frequency region. The maximum occurs at a frequency of 690 Hz. The maximum loss of the order of 3100  $\Omega$  is observed in pure stilbite. For  $\text{TiO}_2$ /Stilbite composites, the change of imaginary part of impedance ( $Z''$ ) as a function of real part ( $Z'$ ) as presented in Fig. 8.(c-d), depicts the presence of high frequency arcs with low frequency branches. The semicircle part of graph exist in higher frequency side and tail is toward lower frequency side. As concentration of  $\text{TiO}_2$  increases in main matrix, tail part of plots goes on

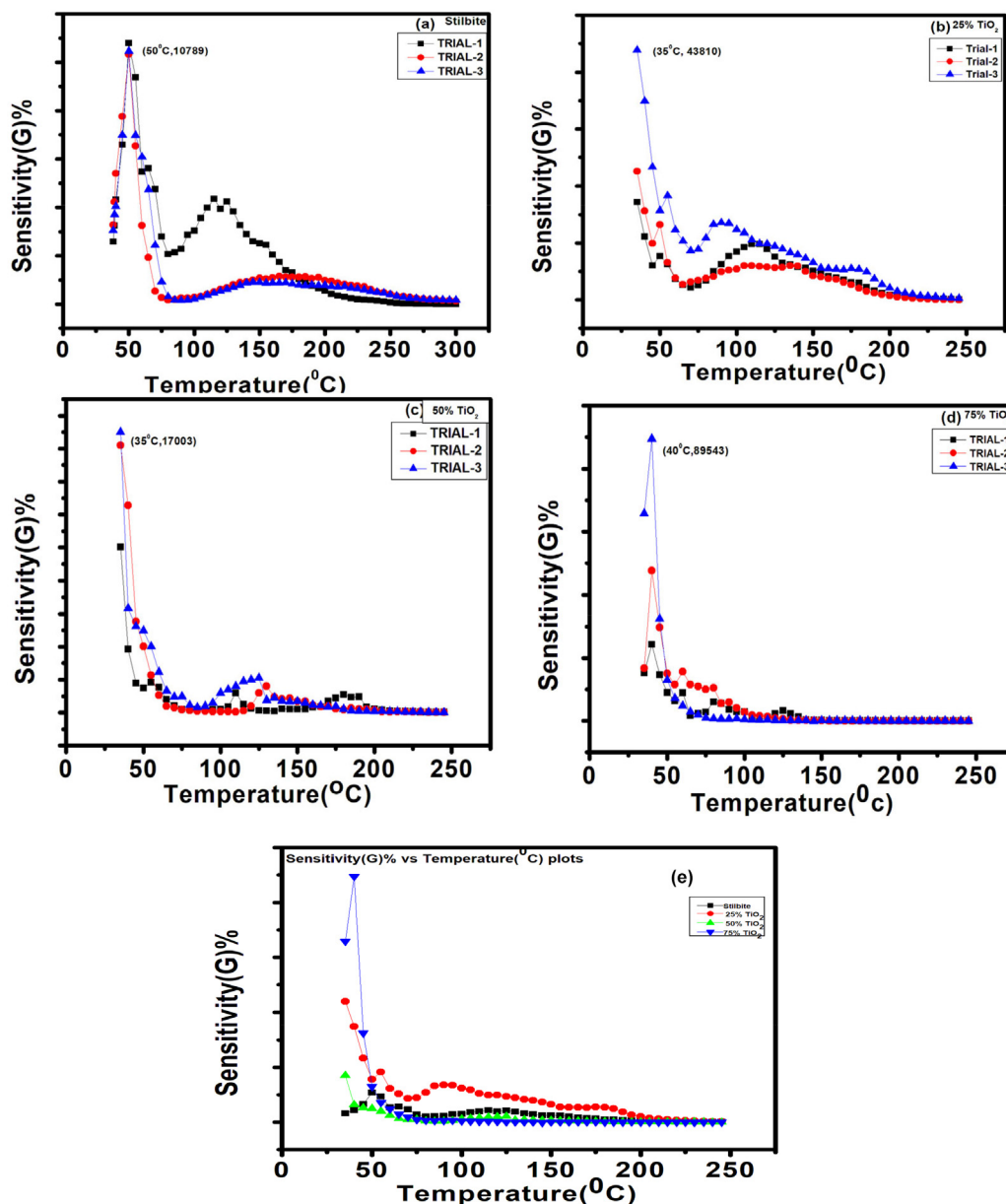


Fig. 3. Repeatability of stilbite and TiO<sub>2</sub>/Stilbite composite-a) stilbite b)25% TiO<sub>2</sub> c) 50%TiO<sub>2</sub> d) 75% TiO<sub>2</sub>.e. Comparison of ammonia response by stilbite and TiO<sub>2</sub> /Stilbite composite showing shift in operating temperature.

Table 1

Gas sensing parameters of stilbite and stilbite composites.

Gas sensing parameter/Materials	Pure Stilbite	25% TiO <sub>2</sub>	50% TiO <sub>2</sub>	75% TiO <sub>2</sub>
Operating temperature(°c)	50	35	35	40
Response time(Sec)	540	360	294	233
Recovery time(Sec)	60	341	254	220
Sensitivity	17,250	43,932	17,015	89,423
Gas uptake capacity(ppm)	100	1100	300	1300

increasing. Low frequency sides correspond to the interfacial impedance and high frequency region can be assigned to bulk impedance. As the concentration of TiO<sub>2</sub> rises, the loss is observed to be reducing. The location of maxima are also found to be dependent on TiO<sub>2</sub> concentration.

The variation of ac conductivity with frequency for TiO<sub>2</sub>/Stilbite composites (depicted in Fig. 9). It show frequency independent behaviour in low frequency region. However, the value of ac con-

ductivity increases in high frequency region where the conductivity deviates from the plateau region[27]. This may be due to hopping of charge carriers in finite cluster. Same trend is shown by all composites. The dielectric study reveals that dielectric constant, cole-cole plots, ac conductivity are the functions of concentration of TiO<sub>2</sub> filler in composites. TiO<sub>2</sub>/Stilbite composites can be called as high-k materials.

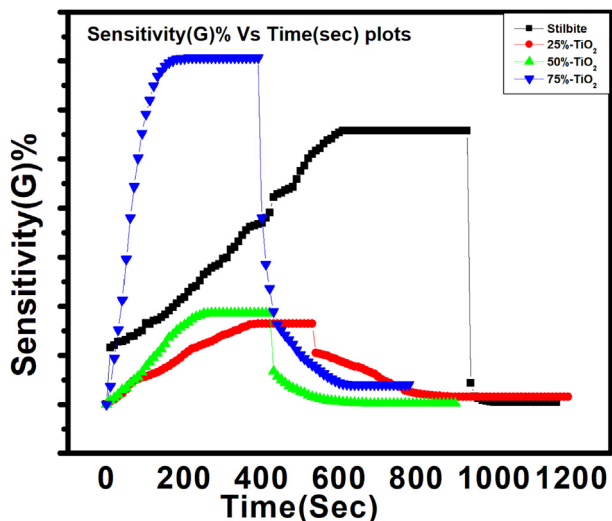


Fig. 4. Comparative study of change in ammonia response as a function of time gives the response and recovery time.

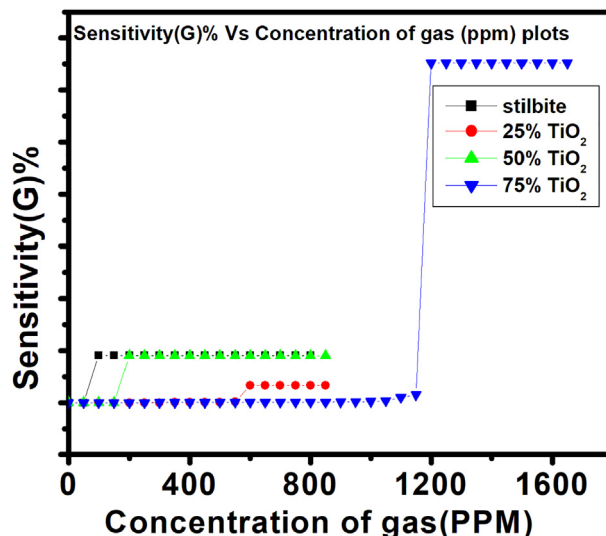


Fig. 6. Comparison of ammonia adsorption capacity of Stilbite and TiO<sub>2</sub>/Stilbite composites as function of ammonia concentration in ppm.

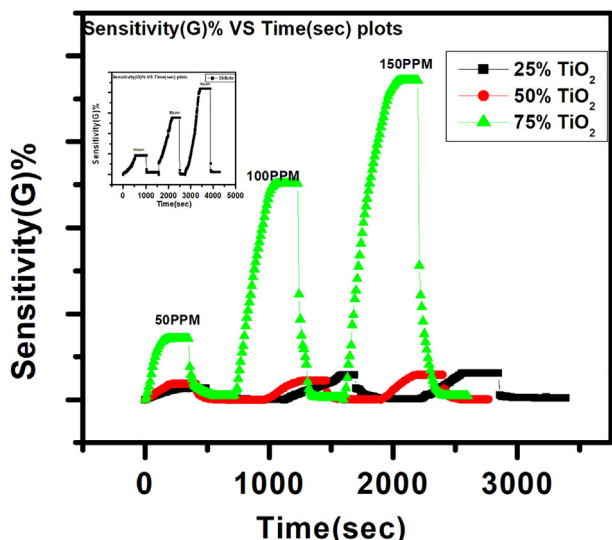


Fig. 5. Comparative study of transient behaviour for Stilbite and its composites.

The dielectric parameter of stilbite and its composites are shown in following Table 2.

#### 4. Conclusion

The composites of stilbite with metal oxide TiO<sub>2</sub> have been developed by physical process. The XRD and FTIR revealed the successful addition of TiO<sub>2</sub> in stilbite. The composite with 75% TiO<sub>2</sub>-25% stilbite composite shows very good result compared to stilbite and rest of the composites. This composite shows maximum sensitivity, highest gas uptake capacity, fast response time with operating temperature of 40 °C. The dielectric constant of these composite increases remarkably compared to pure stilbite. Thus 75% TiO<sub>2</sub>-25% stilbite composite is good ammonia gas sensor and dielectric materials/

#### CRedit authorship contribution statement

**Kutte Vikas** : Kishori Naik: Data curation. **Madhuri Lakhane**: Formal analysis. **Wakade Malikarjun** : **Pankaj Waghmare**: Data

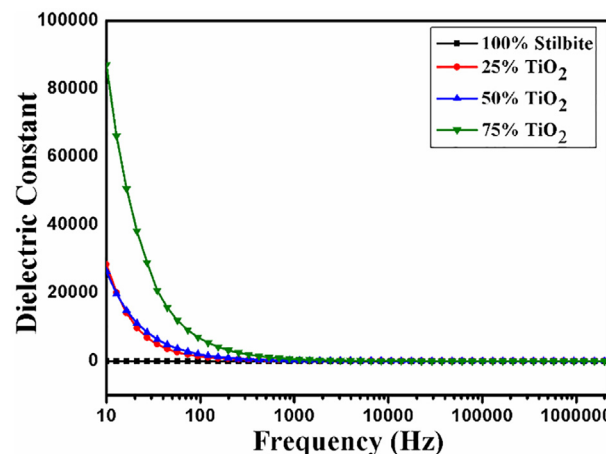


Fig. 7. (a-c).Variation of dielectric constant of stilbite and TiO<sub>2</sub>/stilbite composite with frequency of applied AC field.

curation, Software. **Pandurang Sabale**: Visualization. **Megha Mahabole**: Supervision, Writing – original draft, Writing – review & editing.

#### Data availability

The data that has been used is confidential.

#### Declaration of Competing Interest

The authors declare the following financial interests/personal relationships which may be considered as potential competing interests: Megha P. Mahabole reports administrative support was provided by Swami Ramanand Teerth Marathwada University, Nanded. Vikas Dhondiba Kutte reports a relationship with Yeshwant Mahavidyalaya Nanded that includes: employment. Vikas Dhondiba Kutte has patent No pending to No.

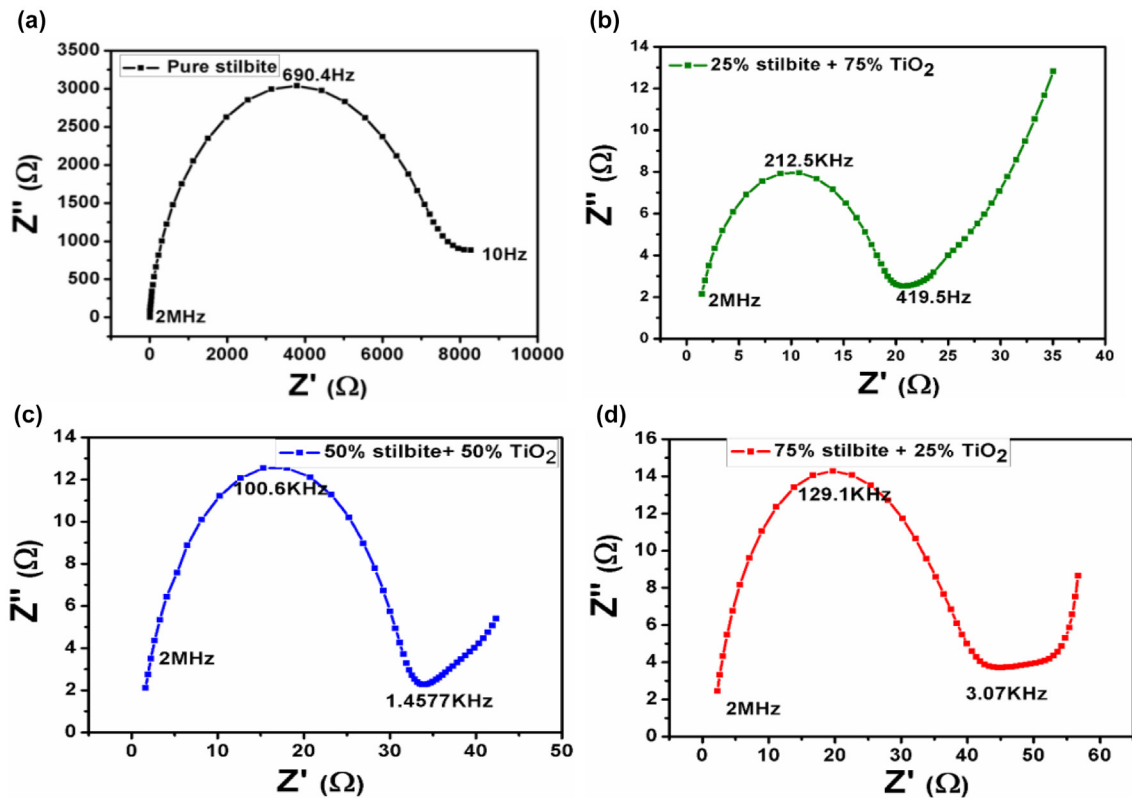


Fig. 8. (a-d). Complex impedance plots of pure stilbite and metal oxide TiO<sub>2</sub>/stilbite samples with variable concentrations; a)Pure stilbite b)25%TiO<sub>2</sub> c) 50%TiO<sub>2</sub> d) 75%TiO<sub>2</sub>.

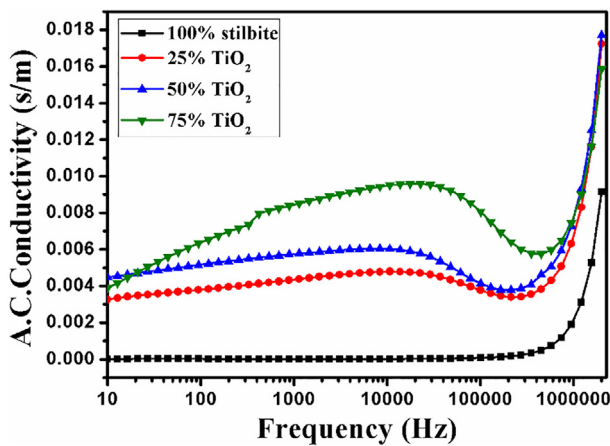


Fig. 9. Variation of AC Conductivity(s/m) of stilbite and its composites versus applied AC frequency.

**Acknowledgement**

Authors would like to acknowledge Hon. Vice Chancellor of Swami Ramanand Teerth Marathwada University, Nanded for his continuous support and encouragement.

**Table 2**

Dielectric properties of stilbite and its composites.

Dielectric parameter/Materials	Pure Stilbite	25% TiO <sub>2</sub>	50% TiO <sub>2</sub>	75% TiO <sub>2</sub>
Dielectric Constant	14	28,454	26,348	87,094
Ac conductivity(s/m)	0	0.00325	0.0045	0.004

**References**

- [1] Frumkin, " American journal of preventive medicine 35.5" (2008): 403-410.
- [2] Wetchakun, " Sensors and Actuators B: Chemical 160.1" (2011): 580-591.
- [3] Giddey, " International Journal of Hydrogen Energy 38.34" (2013): 14576-14594
- [4] Timmer, " Sensors and Actuators B: Chemical 107.2" (2005): 666-677
- [5] Peel, " Journal of Biogeochemistry 114.1" (2013): 121-134
- [6] Xianhui, " The Chemistry of Nanostructured Materials." 2003. 1-37
- [7] Flanigen, " Pure and applied chemistry 52.9 (1980): 2191-2211.
- [8] Hussain, " Current Analytical Chemistry 17.1" (2021): 82-97.
- [9] Pires, " Microporous and Mesoporous Materials 43.3 (2001): 277-287
- [10] Kesraoui-Ouki, " Journal of Chemical Technology & Biotechnology 59.2" (1994): 121-126
- [11] Lakhane, " procedia Technology 24 (2016): 595-602.
- [12] Y. Sun, " J. Desalin." 277 (1-3) (2011) 121-127.
- [13] Baek, " Journal of Microporous and Mesoporous Materials", (2018), 264, 159-166.
- [14] Kiseleva, " Journal of American Mineralogist", (2001). 86(4), 448-455
- [15] Schäfer, " Journal of electroceramics 16" (2006): 93-98.
- [16] Tomchenko, " Sensors and Actuators B: Chemical 93.1-3" (2003): 126-134
- [17] Marquis, " Sensors and Actuators B: Chemical 77.1-2" (2001): 100-110
- [18] Meixner, " Journal of Sensors and Actuators B: Chemical 23.2-3" (1995): 119-125
- [19] Wang, " Journal of Sensors 17.9" (2017): 1971.
- [20] Lakhane, " Nano-Structures & Nano-Objects 17" (2019): 248-258.
- [21] Mahabole, " Indian Journal of Physics 89.2" (2015): 167-174
- [22] Gracia, " The Journal of Physical Chemistry C 117.30" (2013): 15659-15666.
- [23] Rawat, " Advanced Materials Letters 3.4" (2012): 286-292.
- [24] Feng, " Journal of Analytical and Applied Pyrolysis 118" (2016): 9-19.
- [25] Lakhane, " Nano-Structures & Nano-Objects 17 (2019): 248-258
- [26] Mahabole, " Journal of Physics: Conference Series. Vol. 1913. No. 1, IOP Publishing", 2021...
- [27] M. Hashim et al., Physica B: Condens. Matter 407 (21) (2012) 4097-4103.